Cranial irradiation impairs intrinsic excitability and synaptic plasticity of hippocampal CA1 pyramidal neurons with implications for cognitive function

https://doi.org/10.4103/1673-5374.336875

Date of submission: July 4, 2021

Date of decision: August 20, 2021

Date of acceptance: December 3, 2021

Date of web publication: February 28, 2022

Min-Yi Wu[1, #], Wen-Jun Zou[2, #], Pei Yu[1, #], Yuhua Yang[1], Shao-Jian Li[1], Qiang Liu[1], Jiatian Xie[1], Si-Qi Chen[3], Wei-Jye Lin[4, 5, 6, *], Yamei Tang[1, 4, 6, *]

From the Contents

Graphical Abstract *The hippocampal CA1 pyramidal neurons are susceptible to radiation-induced long-term impairment of the intrinsic electrophysiology and synaptic plasticity*

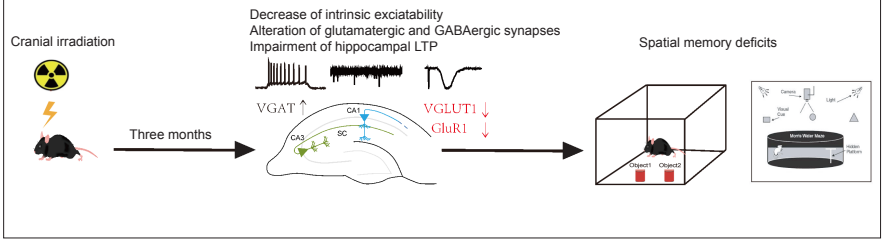

Abstract

Radiation therapy is a standard treatment for head and neck tumors. However, patients often exhibit cognitive impairments following radiation therapy. Previous studies have revealed that hippocampal dysfunction, specifically abnormal hippocampal neurogenesis or neuroinflammation, plays a key role in radiation-induced cognitive impairment. However, the long-term effects of radiation with respect to the electrophysiological adaptation of hippocampal neurons remain poorly characterized. We found that mice exhibited cognitive impairment 3 months after undergoing 10 minutes of cranial irradiation at a dose rate of 3 Gy/min. Furthermore, we observed a remarkable reduction in spike firing and excitatory synaptic input, as well as greatly enhanced inhibitory inputs, in hippocampal CA1 pyramidal neurons. Corresponding to the electrophysiological adaptation, we found reduced expression of synaptic plasticity marker VGLUT1 and increased expression of VGAT. Furthermore, in irradiated mice, long-term potentiation in the hippocampus was weakened and GluR1 expression was inhibited. These findings suggest that radiation can impair intrinsic excitability and synaptic plasticity in hippocampal CA1 pyramidal neurons.

Key Words: GABA-mediated hyperfunction; GluR; intrinsic excitability; long-term potentiation; radiation-induced cognitive impairment; spontaneous excitatory postsynaptic currents; spontaneous inhibitory postsynaptic currents; synaptic plasticity; type I vesicular glutamate transporter; vesicular GABA transporter; whole-cell patch clamp recording

Introduction

Radiation therapy is included in established therapeutic protocols used to treat multiple types of head and neck tumors (McTyre et al., 2013; Owonikoko et al., 2014). While cranial radiotherapy has been proven to significantly extend the survival rate of cancer patients, the treatment is routinely associated with serious complications, including cognitive impairment. Indeed, 6 months to 1 year after radiation, 50–90% of patients exhibit cognitive dysfunction that severely affects their quality of life (Greene-Schloesser et al., 2013; Makale et al., 2017). However, the mechanisms by which radiation induces cognitive dysfunction have not been thoroughly elucidated.

The hippocampus has long been considered a pivotal brain area for learning and memory (Bartsch and Wulff, 2015; Wang et al., 2020, 2021; Xue et al., 2021). Structural and functional changes in the hippocampus can result in increased vulnerability to pathological states associated with cognitive deficits (Galvin et al., 1999; von Oertzen et al., 2002; Blum et al., 2012). Notably, patients receiving brain irradiation exhibited deficits in learning and spatial processing, which are related to hippocampal function (Gondi et al., 2010), while hippocampus-avoidance radiotherapy has been found to preserve cognitive function (Andreas and Kundapur, 2015; Brown et al., 2020). Several studies have reported that the hippocampus is vulnerable to radiation, and have linked radiation-induced structural changes in the hippocampus to cognitive decline (Galvin et al., 1999; Rao et al., 2011; Son et al., 2015). Researchers have also reported that deficits in hippocampal neurogenesis (Monje et al., 2002; Zou et al., 2012) and neuroinflammation (Peng et al., 2014; Montay-Gruel et al., 2019) played critical roles in radiation-induced cognitive impairment (Son et al., 2015). However, radiation-induced electrophysiological adaptation in hippocampal neurons has not been well characterized.

Here, we investigated the long-term impact of a single radiation dose of 30 Gy on the intrinsic electrophysiology and synaptic plasticity of hippocampal CA1 pyramidal neurons. Our findings provide new insights regarding the pathogenic mechanisms underlying radiation-induced cognitive deficits.

[1]Department of Neurology, Sun Yat-sen Memorial Hospital, Sun Yat-sen University, Guangzhou, Guangdong Province, China; [2]State Key Laboratory of Organ Failure Research, Key Laboratory of Mental Health of the Ministry of Education, Guangdong-Hong Kong-Macao Greater Bay Area Center for Brain Science and Brain-Inspired Intelligence, Key Laboratory of Psychiatric Disorders of Guangdong Province, Collaborative Innovation Center for Brain Science, Department of Neurobiology, Southern Medical University, Guangzhou, Guangdong Province, China; [3]Department of Anesthesiology, Sun Yat-sen Memorial Hospital, Sun Yat-sen University, Guangzhou, Guangdong Province, China; [4]Guangdong Provincial Key Laboratory of Malignant Tumor Epigenetics and Gene Regulation, Guangdong-Hong Kong Joint Laboratory for RNA Medicine, Sun Yat-sen Memorial Hospital, Sun Yat-sen University, Guangzhou, Guangdong Province, China; [5]Medical Research Center, Sun Yat-sen Memorial Hospital, Sun Yat-sen University, Guangzhou, Guangdong Province, China; [6]Guangdong Province Key Laboratory of Brain Function and Disease, Zhongshan School of Medicine, Sun Yat-sen University, Guangzhou, Guangdong Province, China

***Correspondence to:** Wei-Jye Lin, PhD, linwj26@mail.sysu.edu.cn; Yamei Tang, MD, PhD, tangym@mail.sysu.edu.cn.

https://orcid.org/0000-0002-6353-6107 (Yamei Tang); https://orcid.org/0000-0002-8392-7121 (Min-Yi Wu)

#These authors contributed equally to this work.

Funding: *This work was supported by the National Natural Science Foundation of China, Nos. 81925031 (to YT), 81820108026 (to YT), 81972967 (to WJL), 81872549 (to YL); the Youth Program of National Natural Science Foundation of China, No. 81801229 (to YTX); a grant from Guangdong Science and Technology Department of China, Nos. 2020B1212060018 (to WJL), 2020B1212030004 (to WJL); the Natural Science Foundation of Guangdong Province, No. 2019A1515011754 (to WJL); the Science and Technology Program of Guangzhou of China, No. 202007030001 (to YT); and the Science and Technology Planning Project of Guangzhou of China, No. 201704030033 (to YL).*

How to cite this article: *Wu MY, Zou WJ, Yu P, Yang Y, Li SJ, Liu Q, Xie J, Chen SQ, Lin WJ, Tang Y (2022) Cranial irradiation impairs intrinsic excitability and synaptic plasticity of hippocampal CA1 pyramidal neurons with implications for cognitive function. Neural Regen Res 17(10):2253-2259.*

Materials and Methods

Animals

Adult 8- to 10-week-old C57BL/6J special pathogen free-level male mice (n = 40) weighing 20–25 g were used for all experiments. The mice were obtained from Guangdong Medical Laboratory Animal Center (Guangzhou, China; license No. SCXK (Yue) 2021-0029). All mice were maintained on a 12-hour light-dark circadian cycle and had free access to food and water in a suitable environment with a temperature of 18–22°C and humidity of 50–60%. The mice were monitored on a daily basis and weighed every 7 days to ensure that the experimental intervention was well tolerated. This study was approved by the Animal Research Ethics Committee of Sun Yat-sen University (approval No. Bei-B2019-0218QX) on October 21, 2019. All animal care and experimental protocols were conducted following the institutional guidelines of Sun Yat-sen University and the NIH Guide for the Care and Use of Laboratory Animals. Endeavors were made to limit the pain and suffering of the animals used in this study.

Cranial irradiation

The protocol for irradiation of mice has been previously described (Xu et al., 2015). Briefly, adult male mice were separated randomly into control and radiation groups. Cranial irradiation of the mice was performed using a 6 MV β-ionizing-ray linear accelerator (Siemens, Munich, Germany). Anesthetized mice were fixed on a custom-designed platform. The mice were positioned such that the treatment field extended from the post-canthus line to the post-aurem line (Xu et al., 2015). The mice in the radiation group received irradiation in a single dose of 30 Gy, delivered at a rate of 3 Gy/min for 10 minutes with a source-to-skin distance of 100 cm. To exclude the possible effects of anesthesia, mice from the control group underwent the same anesthesia procedures as those in the radiation group, but did not receive irradiation. A total of 22 mice received irradiation and 18 mice underwent a sham operation, and the mice came from three separate cohorts. Only 16 mice in the radiation group (6 mice died after irradiation, mortality rate = 27%) and 18 mice in the control group were assessed 3 months after irradiation. One cohort of mice was used for behavioral tests and electrophysiological recording, and the other two cohorts were separately used for electrophysiological recording and tissue collection, respectively. All assessments were conducted 3 months after cerebral irradiation in both the radiation and control groups.

Novel object location test

To examine the long-term memory of mice, we carried out the novel object location test according to previous reports (Leger et al., 2013; Glasgow et al., 2020). After handling the mice daily for 5 days, they were habituated to a square chamber (33 cm × 33 cm × 20 cm) containing no objects for 10 minutes (day 1). On day 2, the animals were exposed to two identical objects in the chamber and given a total exploration time of 10 minutes. On day 3, one of the two objects was relocated to a new position and the animals were allowed to freely explore the chamber for a total of 10 minutes. Mice that did not explore the two objects for at least 20 seconds within the 10-minute period on day 2 or 3 were removed from the analysis. Throughout the entire experiment, an overhead camera was used to record the behavior of the mice in the chamber. The amount of time spent engaged in exploration on days 2 and 3 was measured by a highly experienced observer (JX) who was blinded to the experimental groups. The experimental chamber and objects were cleaned with 70% ethanol to reduce the influence of mouse odor between the trials. The exploration times were defined as the total time during which the mice sniffed each object (2 cm within the object with the nose angled directly toward the object). Recognition ratios were calculated as the amount of time spent sniffing an object, divided by the total time spent exploring both objects.

Morris water maze

To examine the spatial memory of mice, we performed the Morris water maze (MWM) as previously reported (Vorhees and Williams, 2006). A circular pool (110 cm in diameter) was filled with water that was made opaque using non-toxic white paint. The temperature of the pool was set at 20–22°C. In the training phase, which took 5 days, the mice were trained to find a round platform that was submerged 1 cm below the surface of the water in the northeast quadrant of the pool. Each mouse completed four trials per day. The starting point for each trial was either the southeast or northwest quadrant, selected at random. The search time for each trial was 60 seconds. Mice were guided to the platform if they did not find it within 60 seconds, and were allowed to remain on the platform for 15 seconds after each trial. The mice were allowed to rest between the trials for 1 minute. A probe test, in which the platform was absent from the pool, was carried out on day 6. For the probe test, mice were placed in the pool at a novel location (southwest quadrant) and permitted to swim for 60 seconds. We used TopScan^{TM}2.0 (CleverSys, Washington, DC, USA), which is a tracking system with a camera, to calculate escape latency, swimming speed, the percentage of time spent in each quadrant, and the number of crossings into each quadrant. In a cued test, which took place after the probe test, a visible flag was attached to the platform. This allowed us to record the swimming latency for a visible platform.

Electrophysiological recording

The procedures for brain slice preparation and electrophysiological recording were as previously reported (Zou et al., 2020). In brief, mice were quickly decapitated under 1% pentobarbital anesthesia (100 mg/kg, Sigma, St. Louis, MO, USA; intraperitoneal injection). Brains were dissected into ice-cold oxygenated modified artificial cerebrospinal fluid (in mM: 250 sucrose, 26 $NaHCO_3$, 10 glucose, 10 $MgSO_4$, 2 KCl, 1.3 NaH_2PO_4, and 0.2 $CaCl_2$, incubated with 95% O_2 and 5% CO_2). Coronal hippocampal slices (300 μm thick) were prepared using a vibratome (Leica, Heerbrugg, Germany, VT-1200S) and incubated at 34°C for half an hour in oxygenated regular artificial cerebrospinal fluid (in mM: 126 NaCl, 26 $NaHCO_3$, 10 glucose, 3 KCl, 2 $CaCl_2$, 1.25 NaH_2PO_4, and 1 $MgSO_4$). After incubation, the brain slices were placed in a recovery chamber at 25 ± 1°C for one hour and then transferred to the electrophysiological recording area. All extracellular solutions were constantly oxygenated using 95% O_2/5% CO_2. During recording, brain slices were submerged and superfused by normal, oxygenated artificial cerebrospinal fluid solution (2 mL/min) at 32–34°C. Electrophysiological data were recorded using a MultiClamp700B amplifier and analyzed with PClamp software (Molecular Devices, San Jose, CA, USA), followed by filtering at 2 kHz and digitization at 10 kHz using Digidata 1440 (Molecular Devices).

For LTP recording, field excitatory postsynaptic potentials (fEPSPs) from the CA1 stratum radiatum were recorded following stimulation of Schaffer collaterals using a two-concentric bipolar stimulating electrode (FHC, Bowdoin, ME, USA). We defined the strength of synaptic transmission as the initial (10–60% rising phase) slope of the fEPSPs. LTP was induced via a 100-Hz stimulus train with 50 pulses, and signals were recorded for 60 minutes. The level of LTP was determined by the average fEPSPs slope during the last 10 minutes of recording after tetanic stimulation.

To measure the intrinsic excitability of CA1 pyramidal neurons, cells were viewed and selected using an upright microscope (ECLIPSE FN1, Nikon, Tokyo, Japan) with a 40× water-immersion objective and infrared differential interference contrast, as well as a digital camera. Borosilicate glass pipettes with a tip resistance of 3–5 MΩ were prepared using a horizontal pipette puller (P-2000, Sutter Instrument, Novato, CA, USA) and filled with solution (in mM: 105 K-gluconate, 30 KCl, 10 HEPES, 10 phosphocreatine, 4 ATP-Mg, 0.3 GTP-Na, and 0.3 glycol-bis-(2-aminoethylether)-N,N,N′,N′-tetraacetic acid (EGTA), pH 7.35, 285 mOsm). Whole-cell recordings were performed using the current-clamp technique, and spikes were induced by injecting a series of depolarizing current pulses in the presence of 20 μM CNQX (a competitive α-amino-3-hydroxy-5-methyl-4-isoxazole-propionicacid (AMPA)/kainate receptor antagonist), 100 μM DL-AP5 (a N-methyl-D-aspartic acid (NMDA) glutamate site antagonist), and 20 μM bicuculline. The threshold of an action potential (AP) was calculated as the depolarization at which the neuron fired. The rheobase was determined by performing a series of current injections and recording the current that elicited the first spike.

For recording spontaneous excitatory postsynaptic currents (sEPSCs), the neuronal membrane potential was held at –70 mV (using the voltage-clamp technique) in 20 μM bicuculline to block gamma-aminobutyric acid type A ($GABA_A$) receptors. For recording spontaneous inhibitory postsynaptic currents (sIPSCs), the neuronal membrane potential was held at 0 mV (using the voltage-clamp technique) in 20 μM CNQX and 50 μM DL-AP5 to block AMPA receptors and NMDA receptors. The pipettes were filled with solution (in mM: 135 Cs-Meth, 10 KCl, 1 $MgCl_2$, 0.2 EGTA, 2 QX-314, 4 ATP-Mg, 0.3 GTP-Na, and 20 phosphocreatine, pH 7.3), with an mOsm of 290–300. We did not analyze datasets with a maintenance current > –200 pA or a shift in the value resistance of the series > 20%. Datasets were attained using pClAMP10.7 (Molecular Devices), and assessed via Clampfit 10.7® software (Molecular Devices) and Mini Analysis software (Synaptosoft Inc., Leonia, NJ, USA).

Immunofluorescence staining

To examine molecular synaptic plasticity in CA1, the brains were collected from mice after anesthetization via 1% pentobarbital (100 mg/kg, intraperitoneal injection) and intracardiac perfusion with 0.9% saline followed by 4% paraformaldehyde. The brains were post-fixed in 4% paraformaldehyde overnight and then transferred to 20% sucrose in phosphate buffered saline (PBS), followed by 30% sucrose in PBS until they sank to the bottom of the container. We prepared 30 μm-thick coronal sections using a microtome (NX50, Thermo Waltham, MA, USA). Brain slices containing the hippocampus were selected and washed with PBS three times for 5 minutes. After that, sections were incubated with 5% normal donkey serum (Beyotime Biotechnology, Shanghai, China) with 0.4% Triton X-100 for 1 hour at room temperature. After blocking, slices were incubated with a rabbit polyclonal antibody against vesicular GABA transporter (VGAT; 1:500, Cat# 131002, RRID: AB_887871, SySy, Goettingen, Germany) and a polyclonal guinea pig antibody against type I vesicular glutamate transporter VGLUT1; 1:500, Cat# 135304, RRID: AB_887878, SySy) in 1% normal donkey serum solution at 4°C overnight. The brain slices were next incubated with donkey anti-rabbit Alexa Fluor 488-conjugated IgG (1:500, Cat# 711-545-152, RRID: AB_2313584, Jackson ImmunoResearch Labs, Philadelphia, PA, USA) and donkey anti-guinea pig Alexa Fluor 594-conjugated IgG (1:500, Cat#106-585-003, RRID: AB_2337442, Jackson ImmunoResearch Labs) for 2 hours at room temperature, washed with PBS three times (5 minutes each), and covered with Fluoroshield^{TM} with 4,6-diamino-2-phenyl indole (F6057, Sigma). Images were acquired using an LSM 800 confocal microscope (Carl Zeiss, Oberkochen, Germany) with a 20× objective.

Western blot assay

The electrophysiological recordings revealed a significant change in synaptic plasticity. Accordingly, we analyzed changes in the expression of synapse-associated markers, including neurotransmitter vesicular transporters (VGAT and VGLUT1) and neurotransmitter receptors including AMPAR (GluR1 and

GluR2), NMDAR (NMDAε2), and GABAR ($GABA_A$ receptor(α1–6)). Whole hippocampal tissue from the control and radiation groups was isolated and immediately sonicated in 200 μL of radio immunoprecipitation assay buffer (Beyotime Biotechnology, P0013B) containing 1× halt™ protease and a phosphatase inhibitor single-use cocktail (Cat# 78443; Invitrogen, Waltham, MA, USA). The supernatant of the samples was collected after being centrifuged under 4°C at 15,364 × *g* for 15 minutes. Total protein quantification was performed using the Pierce™ BCA Protein Assay Kit (Cat# 23225, Invitrogen). Then, equal amounts (30 μg) of the protein samples were mixed with protein loading buffer, boiled, and analyzed via 10% polyacrylamide gel with 0.1% sodium dodecyl sulfate. The proteins were transferred to polyvinylidene fluoride membranes (0.2 μm, Merch Millipore, Carrigtwohill, Ireland), followed by 5% milk-blocking for 60 minutes at room temperature in Tris-buffered saline (TBS)/0.1% Tween-20, and consequently transferred in the presence of primary antibodies (see below) to TBS/0.1% Tween-20 overnight at 4°C. Following three 8-minute washes with TBS/0.1% Tween-20, the polyvinylidene fluoride membranes were incubated with goat anti-mouse secondary horseradish peroxidase-linked antibodies (1:5000, Cat# 7074S, RRID: AB_2099233, Cell Signaling Technology, Boston, MA, USA) or horse anti-rabbit secondary horseradish peroxidase-linked antibodies (1:5000, Car# 7076S, RRID: AB_330924, Cell Signaling Technology) for an hour at room temperature. Protein signals were visually identified through Clarity Western electrochemiluminescence substrate (Millipore, WBKLS0500) on a chemiluminescence apparatus (Tanon-5200C, Shanghai, China). Quantification was performed using ImageJ Fiji (https://imagej.net/software/fiji/). Primary antibodies used were: mouse antiα-tubulin (1:5000, Cat# 66031-1, RRID: AB_11042766, Proteintech, Rosemont, IL, USA), rabbit anti-VGAT (1:1000, Cat# 131002, RRID: AB_887871, SySy), mouse anti-VGLUT1 (1:1000, Cat# sc-377425, RRID: AB_2687960, Santa Cruz Biotechnology, Santa Cruz, CA, USA), mouse anti-GluR1 (1:1000, Cat# sc-55509, RRID: AB_629532, Santa Cruz Biotechnology), mouse anti-GluR2 (1:1000, Cat# sc-517265, Santa Cruz Biotechnology), mouse anti-NMDAε2 (1:1000, Cat# sc-365597, RRID: AB_10847218, Santa Cruz Biotechnology), and mouse anti-GABAA receptor(α1–6) (1:1000, Cat# sc-376282, RRID: AB_10988210, Santa Cruz Biotechnology).

Statistical analysis

We employed GraphPad Prism 6.0 (GraphPad Software, San Diego, CA, USA) for statistical analyses. The experimental data were represented using dot-blot figures, with error bars showing the mean ± standard error of mean (SEM). The observer was blinded to the experimental groups only for the electrophysiological data. Statistical significance was set at $P < 0.05$. We used independent sample *t*-tests for two-group comparisons. To assess between-group differences in escape latency in the training phase of the behavioral tests, and the differences in the number of spikes fired across a range of current injections, we used a two-way analysis of variance for repeated measures with Sidak's multiple comparisons test.

Results

Radiation induces hippocampus-dependent memory deficits

To assess radiation-induced cognitive impairment, adult male mice that received a single 30 Gy dose of ionizing cerebral irradiation were subjected to tests of cognitive function at 3 months post-irradiation. These tests included the novel object location test and the MWM, which are both hippocampus-dependent memory tasks (**Figure 1A**). In the novel object location test (**Figure 1B**), the radiation and control mice spent an equal amount of time exploring both objects on day 2 (**Figure 1C**). The control mice spent more time exploring the re-located object on day 3 ($P < 0.0001$), while the radiation mice spent an equal amount of time exploring the two objects ($P = 0.335$; **Figure 1D**).

For the MWM test, the mice were trained daily for 5 days to locate the hidden platform. The escape latency (the time taken to find the hidden platform) was longer in the radiation mice compared with the control mice on days 2 ($P < 0.001$) and 3 ($P < 0.001$; **Figure 1E**), but there were no differences between these two groups on days 4 and 5. On day 6, the mice swam in the maze for 60 seconds during the probe test. The swimming patterns during the probe test are illustrated in **Figure 1F**. Compared with the radiation mice, the control mice spent a significantly different amount of time in the different quadrants ($P < 0.0001$), with the longest time spent in the target quadrant (**Figure 1G**). In contrast, the radiation mice spent a similar time amount of time in all of the quadrants ($P = 0.1979$; **Figure 1G**). Moreover, the radiation mice spent significantly less time exploring the target quadrant ($P = 0.0281$; **Figure 1G**) and performed fewer crossings of the previous site of the hidden platform compared with those in the control group ($P = 0.0051$; **Figure 1H**). These data indicate that at three months post irradiation, the mice displayed a spatial memory deficit in the MWM test. We also conducted the cued test (visible platform) and found no significant between-groups difference in the time taken to reach the visible platform ($P = 0.3369$; **Figure 1I**). Furthermore, the two groups had a similar mean swimming speed (**Figure 1J**). This suggests that the radiation did not affect visual or sensorimotor function in the mice. Taken together, these data indicate that a 30 Gy dose of radiation induced long-term spatial memory deficits in mice.

Radiation diminishes excitability of hippocampal CA1 pyramidal neurons

Given that the radiation mice showed hippocampal-dependent memory deficits, we used whole-cell patch clamp recording to assess whether cranial irradiation changed the intrinsic excitability of CA1 pyramidal neurons. CA1 pyramidal neurons from radiation mice exhibited a significant reduction in firing rate compared with those in the control mice ($P = 0.0004$; **Figure 2A** and **B**). We observed an increase in rheobase in the radiation group compared with the control group ($P = 0.0005$; **Figure 2C**), while the AP threshold ($P = 0.3196$; **Figure 2D**) and resting membrane potential ($P = 0.3197$; **Figure 2E**) remained unchanged. We further examined alterations in neuronal excitability by calculating the AP latency and the amount of APs induced by depolarizing current ramps (steps from 0 to 160 pA within a 5-second duration) (**Figure 2F**). Similarly, we found that radiation decreased the total number of APs ($P = 0.0006$; **Figure 2G**) and increased the AP latency ($P = 0.0003$, **Figure 2H**), compared with the mice in the control group. These results indicate that radiation reduced the intrinsic excitability of CA1 pyramidal neurons.

Radiation reduces spontaneous excitatory transmission but increases spontaneous inhibitory transmission to hippocampal CA1 pyramidal neurons

To examine radiation-associated alterations in the excitatory input to hippocampal CA1 pyramidal neurons, we recorded AMPA receptor ($AMPA_R$)-mediated sEPSCs ($V_{hold} = -70$ mV) (**Figure 3A**). The results showed that compared with the control group, the mean sEPSC frequency but not the amplitude in the radiation group was considerably reduced (frequency: $P = 0.018$, amplitude: $P = 0.7038$; **Figure 3B**). We also recorded GABA receptor-mediated sIPSCs ($V_{hold} = 0$ mV) (**Figure 3C**) to enable a functional analysis of inhibitory synapses. We observed a significant enhancement in the mean frequency but not the amplitude of sIPSCs in the radiation group compared with the control group (frequency: $P = 0.0302$, amplitude: $P = 0.7725$; **Figure 3D**). All of these findings suggest that radiation reduced excitatory synaptic input and enhanced inhibitory input to hippocampal CA1 pyramidal neurons.

Radiation impairs hippocampal LTP

LTP is characterized by the persistent strengthening of synaptic activities, and has been associated with learning and memory (Titley et al., 2017). To determine the impact of radiation on synaptic plasticity, we recorded fEPSPs at Schaffer collaterals to CA1 synapses (**Figure 4A**). The input-output curves of the fEPSPs indicated that the radiation did not affect basal synaptic transmission (**Figure 4B**). We then recorded LTP for 60 minutes following one train of high-frequency stimulation (100 Hz with 50 pluses) (**Figure 4C**). In the radiation mice, we observed a significant descent in the fEPSP slope in the last 10 minutes compared with the control mice ($P = 0.0284$; **Figure 4D**). Our results indicate that exposure to cranial irradiation impairs LTP/synaptic plasticity in hippocampal CA1 neurons in mice.

Radiation induces molecular alterations in glutamatergic and GABAergic synapses in the hippocampus

Based on the above electrophysiological findings, we investigated the molecular mechanisms that contributed to the imbalance in excitatory and inhibitory synaptic input after radiation (**Figure 5A**). We first investigated the expression levels of VGLUT1 and VGAT in hippocampal CA1 neurons, which are regarded as excitatory and inhibitory presynaptic markers, respectively (Sando et al., 2017). Interestingly, immunofluorescence staining revealed a dramatic decline in VGLUT1-positive expression and an increase in VGAT-positive expression in hippocampal CA1 neurons in both the pyramidal layer and stratum radiatum in the radiation versus control group (**Figure 5B** and **C**). We further confirmed similar molecular changes in VGLUT1 ($P = 0.0485$) and VGAT ($P = 0.0054$) in the hippocampus via western blot analysis (**Figure 5D–G**). Western blot analysis of other neurotransmitter receptors that are vital to synaptic plasticity indicated a notable decrease in GluR1 expression ($P = 0.0434$; **Figure 5G** and **H**), which is a subunit of AMPAR, but not in GluR2 ($P = 0.7871$; **Figure 5G** and **I**), NMDAε2 ($P = 0.5459$; **Figure 5G** and **J**) or $GABA_A$ receptor(α1–6) ($P = 0.9738$; **Figure 5G** and **K**) expression in the radiation group compared with the control group. In summary, our data indicated that the radiation mice exhibited significant alterations in synaptic markers of glutamatergic and GABAergic neurons in the hippocampus, providing mechanistic clues regarding the long-term effects of radiation with respect to neuronal dysfunction and cognitive impairment.

Discussion

Although cognitive deterioration after cranial irradiation is extensive and devastating, the mechanisms underlying the cognitive sequelae remain largely undetermined (Greene-Schloesser et al., 2013; Makale et al., 2017). Here, we identified changes in cognitive function, pathological characteristics, electrophysiological activity in hippocampal neurons, and associated molecular changes induced by a single 30 Gy dose of radiation in male mice. Our findings offer mechanistic insight regarding cognitive dysfunction following cranial irradiation, suggesting new avenues for therapeutic intervention.

The pathogenesis of irradiation-induced cognitive impairment depends on multiple factors, including the type of radiation used, radiation dose, and whether the treatment was single or fractionated (Bender, 2012; Boria and Perez-Torres, 2019; de Kruijff, 2020), as well as biological sources of variance such as genetic susceptibility (Wang et al., 2019) and sex-based differences (Hinkle et al., 2019; Boria and Perez-Torres, 2020). All of the findings in this study are based on male mice, which represents a limitation regarding the applicability of our data on the effects of cranial irradiation on the intrinsic excitability and synaptic plasticity to female mice. Although most previous animal studies of radiation-induced brain injury have used male animals, recent reports have demonstrated sex differences in the effects of cranial irradiation on cognitive dysfunction, brain necrosis, and spine loss (Hinkle et al., 2019; Boria and Perez-Torres, 2020). Thus, future studies are needed to investigate the influence of sex on the effects of radiation-induced brain injury.

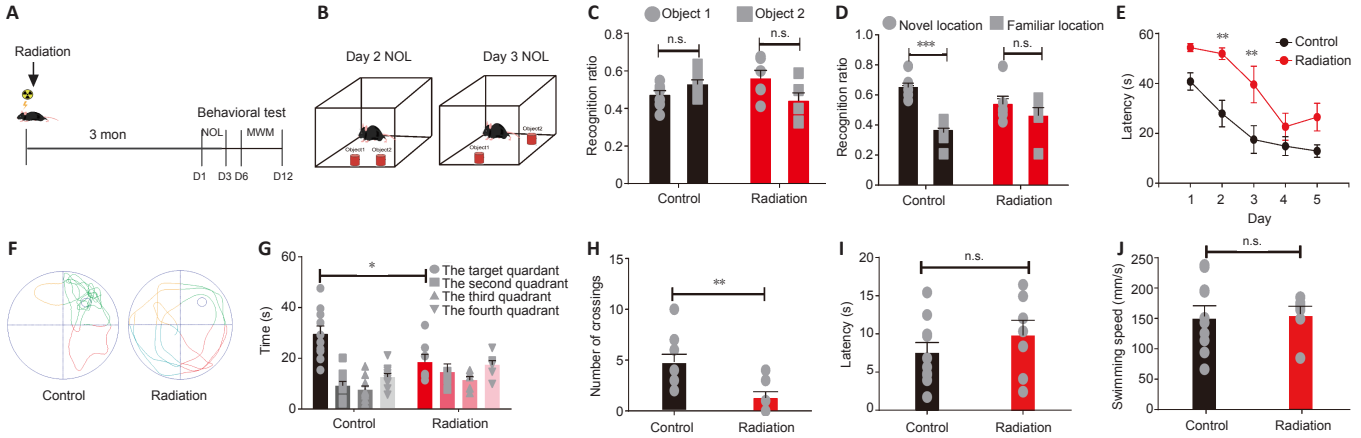

Figure 1 | Mice showed impaired spatial memory performance in the novel object location test (NOL) and the Morris water maze test (MWM) 3 months after a 30 Gy dose of radiation.

(A) Timeline of the NOL and MWM tests. (B) Schematic representation of the NOL. (C) The control and radiation mice were not significantly different in terms of the recognition ratio between objects on day 2 (control: n = 7, independent sample t-test, P = 0.1222; radiation: n = 6, independent sample t-test, P = 0.0772). (D) The control mice had a higher recognition ratio for the relocated object on day 3, while this was not the case for the radiation mice (control: n = 7, independent sample t-test, P < 0.0001; radiation: n = 6, independent sample t-test, P = 0.3335). (E) The escape latency curve during the 5 training days (control/radiation: n = 10/7; two-way repeated measures analysis of variance: time: P < 0.0001; group: P = 0.0009; Sidak's multiple comparisons test: escape latency on day 2: P < 0.01, day 3: P < 0.01; other days: n.s.). (F) Illustration of the swimming pattern in the control and radiation mice during the probe test. (G) The time spent in each quadrant during the probe test (control/radiation: n = 10/7, unpaired Student's t-test, P = 0.0281). (H) Number of crossings of the location of the hidden platform during the probe test (control/radiation: n =10/7, independent sample t-test, P = 0.0051). (I, J) The escape latency to the platform (I: control/radiation: n = 10/7; independent sample t-test, P = 0.3369) and the swimming velocity during the cued test (J: control/radiation: n = 10/7, independent sample t-test, P = 0.8728). Data are expressed as mean ± SEM. *P < 0.05, **P < 0.01, ***P < 0.001. n.s.: No significance.

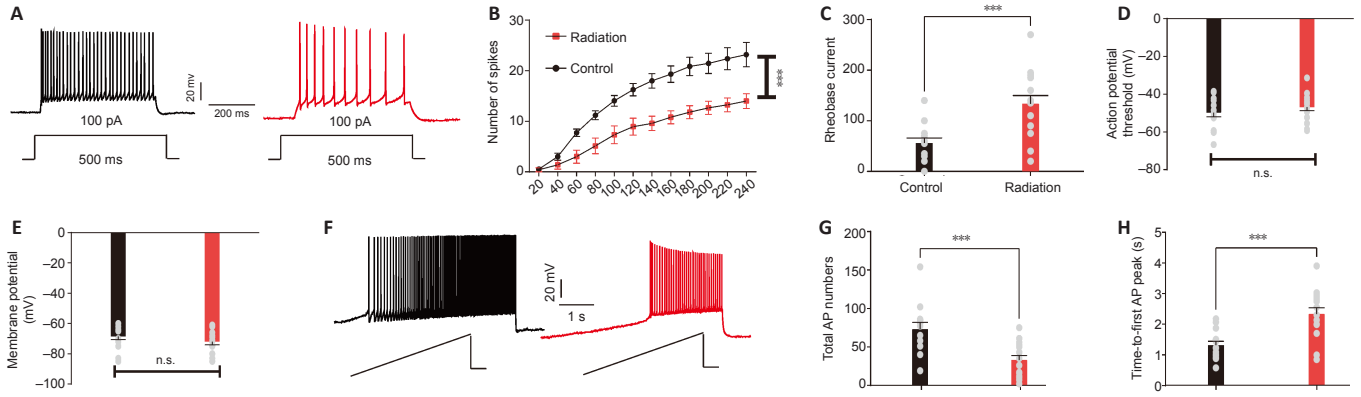

Figure 2 | Radiation diminished intrinsic excitability in hippocampal CA1 pyramidal neurons.

(A) Representative firing patterns of hippocampal CA1 pyramidal neurons in the control (black) and irradiated (red) mice in response to depolarizing current injections (100 pA). (B) Averaging the number of spikes fired indicated a decrease in excitability after radiation across a range of current injections (control/radiation: n = 15/15, two-way repeated measures analysis of variance: current injection: P < 0.0001, group: P = 0.0004). (C) Increased rheobase current in the radiation mice (control/radiation: n = 14/15, independent sample t-test, P = 0.0005). (D, E) We found no significant difference in the action potential threshold (D: control/radiation: n = 14/15; independent sample t-test, P = 0.3196) or resting membrane potential (E: control/radiation: n = 14/15, independent sample t-test, P = 0.3197) between the groups. (F) Representative firing pattern of hippocampal CA1 pyramidal neurons from the control (black) and irradiated (red) mice in response to a series of depolarizing current ramps (steps from 0 to 160 pA with a 5-second duration). Scale bars: 20 mV (vertical axis), 200 ms (horizontal axis). (G) The total number of APs was decreased in irradiated mice (control/radiation: n = 14/15, independent sample t-test, P = 0.0006). (H) Radiation delayed the time to the first AP peak (control/radiation: n = 14/15, independent sample t-test, P = 0.0003). Data are expressed as mean ± SEM. ***P < 0.001. AP: Action potential; n.s.: no significance.

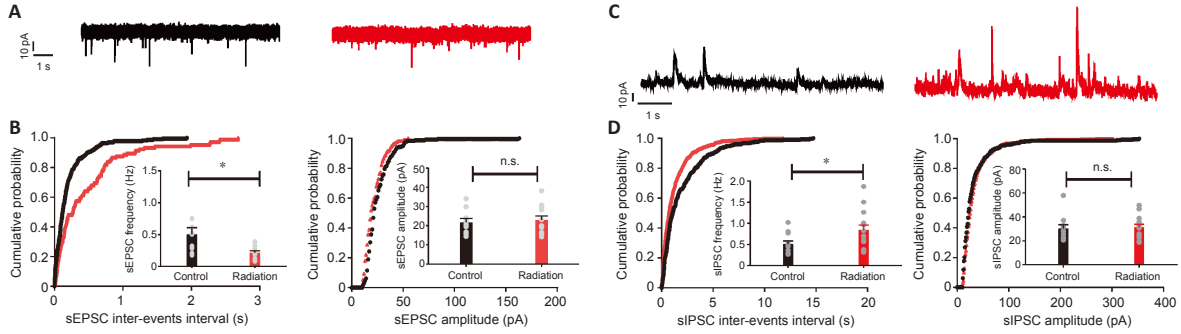

Figure 3 | Radiation decreased the sEPSC and increased the sIPSC in hippocampal CA1 pyramidal neurons.

(A) Representative patterns of sEPSC traces in hippocampal CA1 pyramidal neurons from the control (black) and irradiated (red) mice. (B) Cumulative distribution plots and group data (insert) showed a significant decrease in the average frequency of sEPSCs (left) but not the average amplitude (right) in the irradiated mice (frequency: control/radiation, n = 10/12, independent sample t-test, P = 0.0118; amplitude: control/radiation: n = 10/12, independent sample t-test, P = 0.7038). (C) Representative patterns of sIPSC traces from hippocampal CA1 pyramidal neurons from the control (black) and irradiated (red) mice. (D) Cumulative distribution plots and group data (insert) showed a significant enhancement in the average frequency of sIPSCs (left) but not the average amplitude (right) in the irradiated mice (frequency: control/radiation: n = 11/15, independent sample t-test, P = 0.0302; amplitude: control/radiation: n = 11/15, independent sample t-test, P = 0.7725). Data are expressed as mean ± SEM. *P < 0.05. sEPSC: Spontaneous excitatory postsynaptic current; sEPSC: spontaneous excitatory postsynaptic current.

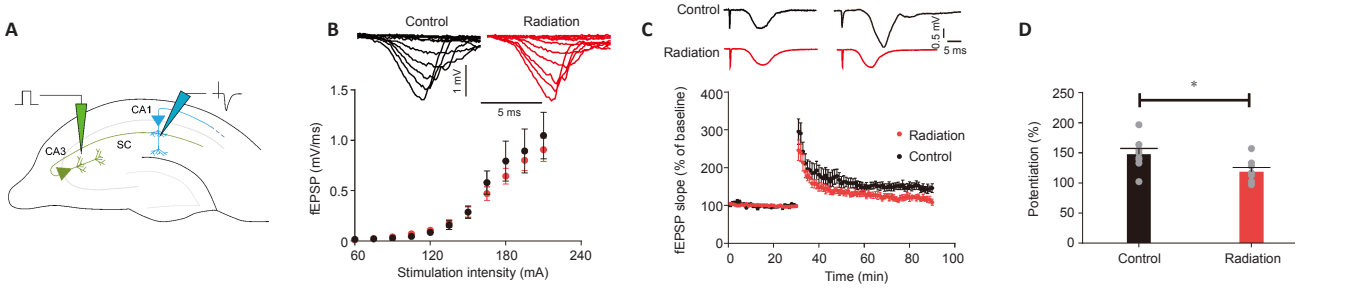

Figure 4 | **Impairment of hippocampal LTP in the irradiated mice.**
(A) Schematic representation of LTP stimulation and recording in hippocampal CA1 and CA3 synapses. (B) Input-output curve of fEPSP slope (n = 8 slices/4 mice in each group). (C) Representative EPSP traces before and 1 hour after high frequency stimulation (100 Hz for 50 pluses) in the control and irradiated mice (upper), the average fEPSP plotted against time in minutes (lower) (n = 4 mice/group). (D) The average fEPSP slopes over the last 10 minutes of recording, normalized to baseline (control/radiation: n = 8/8, independent sample t-test, P = 0.0284). Data are expressed as mean ± SEM. *P < 0.05. EPSP: Excitatory postsynaptic potentials; fEPSPs: field excitatory postsynaptic potentials; LTP: long-term potentiation.

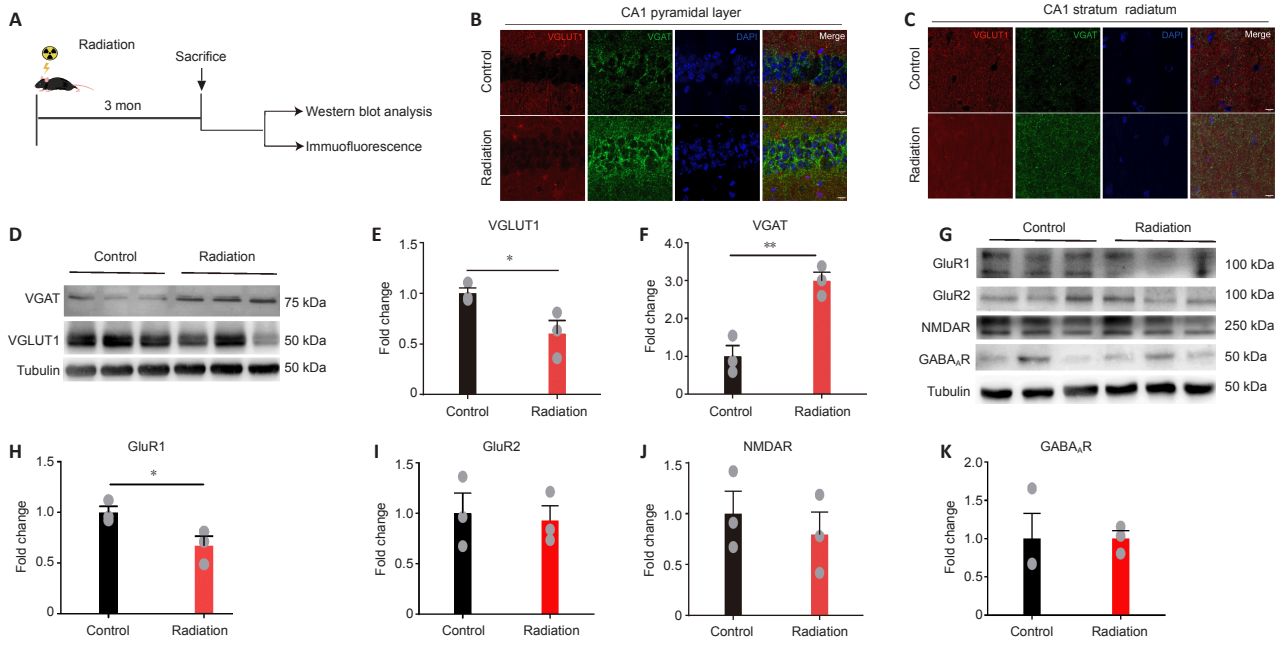

Figure 5 | **Changes in glutamatergic and GABAergic synapses in the hippocampal CA1 of irradiated mice.**
(A) Timeline of western blot and immunofluorescence analysis. (B, C) Radiation induced a decline in VGLUT1 (Alexa Fluor 594 for red) but an increase in VGAT (Alexa Fluor 488 for green) expression in both the pyramidal layer (B) and stratum radiatum (C) of the hippocampal CA1. Scale bars: 10 μm. (D) The expression levels of VGLUT1 increased but those of VGAT decreased in the hippocampus of irradiated mice, as per western blotting, compared with the control mice. (E, F) Quantitative results of VGLUT1 and VGAT expression levels in the hippocampus of control and irradiated mice (control/radiation: n = 3/3, VGLUT1: P = 0.0485, VGAT: P = 0.0054). (G) The expression levels of GluR1, GluR2, NMDAε2, and $GABA_AR$α(1–6) in the hippocampus were evaluated in the control and irradiated mice by western blotting. (H–K) Quantitative results for GluR1, GluR2, NMDAε2, and $GABA_AR$α(1–6) expression levels in the hippocampus for the control and irradiated mice (control/radiation: n =3/3, GluR1: P = 0.0434, GluR2: P = 0.7871, NMDAε2: P = 0.5459, $GABA_AR$α(1–6): P = 0.9738). Data are expressed as mean ± SEM. *P < 0.05, **P < 0.01 (independent sample t-test). $GABA_AR$: γ-Aminobutyrate type A receptor; NMDA: N-methyl-D-aspartic acid; VGAT: vesicular γ-aminobutyrate type A transporter; VGLUT1: type I vesicular glutamate transporter.

In the present study, we used a single instance of irradiation with a high dose in our animal model, as per previous reports (Xu et al., 2015). In animal studies and clinical practice, both single instances of irradiation with a high dose and fractionated irradiation with low dose are used (Yang et al., 2017; Milano et al., 2021). We previously reviewed and summarized the pathophysiological responses to radiation-induced brain injury in different animal models (Yang et al., 2017). Generally, fractionated irradiation carries a reduced risk of developing brain injury in comparison to a single high dose of irradiation. For example, a high cumulative dose (40 Gy) delivered via a fractionated irradiation model did not lead to vascular injury or demyelination at 6 weeks post irradiation (Semmler et al., 2013), and no cognitive deficits persisted after 7 months post irradiation (Lee et al., 2012). However, cranial irradiation delivered in a single high dose has several advantages for studying radiation-induced brain injury, including reproducible and stable phenotypes such as long-term cognitive impairment, vascular damage, white matter changes, and glial activation, which occur within weeks post irradiation (Hodges et al., 1998; Liu et al., 2010).

The type of radiation used is also vital to the pathogenesis of radiation-induced cognitive impairment. Linear energy transfer (LET; expressed as keV/μm) is used to describe the amount of energy deposited per unit of length when radiation passes through a material. High-LET radiation induces more damage per absorbed dose than low-LET radiation. Both high-LET radiation and low-LET radiation can uniquely affect neuroinflammation, neurogenesis, and neuronal morphology in animal models (Manda et al., 2009; Cacao and Cucinotta, 2019; Roobol et al., 2020). For example, altered neurogenesis at the early stage post-irradiation in animal models has been found to vary according to the type or dose of irradiation received (Manda et al., 2009; Rivera et al., 2013; Zanni et al., 2018).

To determine how the hippocampus contributes to radiation-induced cognitive deficits, we examined LTP in the CA1 hippocampal region. In contrast to a previous report on LTP in the dentate gyrus (Wu et al., 2012), we found no detectable change in the Schaffer collateral pathway of the hippocampus during the induction phase of LTP. However, we did find impaired expression of LTP. Importantly, we found that radiation induced a decrease in GluR1 expression in the hippocampus. The AMPAR plays a key role in synaptic plasticity (Malinow and Malenka, 2002; Shepherd and Huganir, 2007), and LTP of synaptic strength is reflected through the synaptic insertion of AMPARs, resulting in synaptic strength enhancement and an increase in spine size (Kopec et al., 2007). Since most of the recruited AMPARs have extrasynaptic origins during LTP formation (Malinow and Malenka, 2002; Patterson et al., 2010), the lack of functional AMPARs on the extrasynaptic surface of GluR1-deficient neurons will result in a major impairment of LTP (Zamanillo et al., 1999; Andrásfalvy et al., 2003; Granger et al., 2013). The radiation-induced loss of GluR1 that we observed in the hippocampus may have led to decreased extrasynaptic AMPARs and weakened synaptic strength, thus further contributing to the functional impairment of LTP expression. One recent report also found a loss of GluR1 expression after radiation (Krishnan et al., 2021), while another showed no detectable changes in GluR1 expression at 12 months post irradiation (Shi et al., 2006), indicating that age and/or time may contribute to the alteration of GluR1 expression after radiation. Radiation-induced impairments in LTP in other hippocampal pathways have also been reported (Zhang et al., 2018). Together with our findings, these

data suggest that radiation may have a direct impact on mature neurons and their function in the hippocampus, partly due to altered GluR1 expression.

GluR1-induced synaptic potentials are the principal contributor to dendritic and somatic depolarization that drives APs (Nicholson and Geinisman, 2009). We found that radiation triggered a prominent decrease in the depolarization-evoked firing activity of CA1 pyramidal neurons compared with non-irradiated neurons. Moreover, the effects of radiation on the intrinsic membrane properties of hippocampal neurons persisted three months post irradiation, resulting in an increased rheobase. A similar alteration in intrinsic electrophysiological properties was found to result in decreased excitability of CA1 pyramidal neurons (Tolliver and Pellmar, 1987; Sokolova et al., 2015), which is likely to affect microcircuit activity in the hippocampus. Moreover, recent reports have shown that radiation altered intrinsic properties of principal cells in the perirhinal cortex (Allen et al., 2020). These results further demonstrate that radiation can directly affect neuronal function.

A balance between excitatory glutamatergic and inhibitory GABAergic transmission in CA1 neurons is indispensable for the proper function of neuronal networks and for normal cognition. We found that exposure to radiation produced a decrease in the frequency of sEPSC in CA1 pyramidal neurons, suggesting that presynaptic glutamate release had decreased. This finding is in agreement with a previous study reporting that radiation led to greater presynaptic versus postsynaptic damage, and that the effect was dose and dose rate dependent and postsynaptic damage required a larger dose of radiation, and was not susceptible to dose rate (Tolliver and Pellmar, 1987; Pellmar et al., 1990). In the present study, we found reduced levels of the presynaptic glutamatergic marker VGLUT1 in the CA1 pyramidal neurons of irradiated mice. Many studies have focused on changes in excitatory synapses after radiation. For instance, an increase in excitatory synapses was observed at the early stage after radiation (< 24 hours) (Duman et al., 2018). However, this acute increase had converted into synapse loss at later time points (> 90 hours) (Duman et al., 2018), and the decrease in spines lasted from days to weeks (Chakraborti et al., 2012; Parihar and Limoli, 2013). These results indicate that radiation ultimately causes an irreversible loss of excitatory synapses, leading to cognitive deficits. Future research is needed to investigate the precise mechanisms driving the conversion from acute increases in excitatory synapses to the loss of excitatory synapses in irradiated brains, and the associated consequences for cognition.

We observed an increase in inhibitory input to CA1 pyramidal neurons in the radiation mice, suggesting that exposure to radiation may increase the probability of GABA release from the synaptic terminal of inhibitory neurons. This result was further confirmed by the increased expression of the inhibitory presynaptic maker VGAT in the irradiated mice. GABA neurotransmission plays a key role in learning/memory processes by modulating synaptic plasticity (Olpe et al., 1993; Huang et al., 2005; Gong et al., 2009), neural oscillations (Gong et al., 2009; Mann and Mody, 2010), and neurogenesis (Ge et al., 2007; Pontes et al., 2013) in the hippocampus. Both GABA-mediated hyperfunction (Clarkson et al., 2010; Zurek et al., 2014; Lissemore et al., 2018; Schulz et al., 2019) and hypofunction (Gill et al., 2011; Han et al., 2014;) can be the primary cause of cognitive impairment in pathological states such as ischemic stroke. Here, we observed an imbalance in the excitatory and inhibitory inputs to CA1 neurons, with significantly increased inhibition. Interestingly, enhanced GABA neurotransmission was also reported in the acute phase (30 minutes) post irradiation (Duman et al., 2018), as well as in 30-day-old irradiated juvenile mice (Caceres et al., 2013). Our findings therefore suggest that reducing GABA-mediated inhibitory neurotransmission in the hippocampus may have therapeutic potential for patients with radiation-induced cognitive impairment. Indeed, this strategy has been effective in treating other neurological diseases (Clarkson et al., 2010; Zurek et al., 2014; Schulz et al., 2019). However, a recent study reported significantly decreased levels of GABA and $GABA_A$ receptors in the hypothalamus after radiation (Franco-Pérez et al., 2020). These studies suggest that the distinct responses to radiation in different brain areas may relate to variations in GABA signaling. There are several types of GABAergic interneurons in the hippocampus. Whether or not there exist cell type-specific interneurons that are sensitive to radiation remains unknown, as we did not observe changes in the expression of $GABA_AR$ expression in the hippocampus of irradiated mice. Additional investigations regarding the molecular mechanisms underlying the enhancement of GABA release from presynaptic terminals are warranted. This study had several limitations. First, we did not examine the molecular mechanisms that modulate the imbalance of excitatory-inhibitory hippocampal neuronal input after cerebral irradiation. Second, we did not examine the mechanisms by which reducing excessive GABA-mediated inhibition by $GABA_A$ receptor antagonists may have therapeutic potential for the treatment of radiation-induced impairments in synaptic plasticity and cognitive function (Fernandez et al., 2007).

In conclusion, we characterized radiation-induced functional alternations in hippocampal neurons, as reflected by changes in intrinsic electrophysiology, synaptic plasticity, and molecular markers. These changes appeared as a long-term consequence of cranial irradiation. Our findings have important implications for understanding the etiology of radiation-induced cognitive impairment and the development of therapeutic strategies for treatment.

Author contributions: *Study design: MYW, WJZ, YT, WJL; experiment implementation: MYW, WJZ, YY, SJL; data analysis: MYW, WJZ, JX, SQC; manuscript draft: MYW, WJZ, YT, WJL, PY, QL. All authors read and approved the final manuscript.*

Conflicts of interest: *There are no conflicts of interest.*

Editor note: YT is an Editorial Board member of Neural Regeneration Research. He was blinded from reviewing or making decisions on the manuscript. The article was subject to the journal's standard procedures, with peer review handled independently of this Editorial Board member and their research groups.

References

Allen BD, Syage AR, Maroso M, Baddour AAD, Luong V, Minasyan H, Giedzinski E, West BL, Soltesz I, Limoli CL, Baulch JE, Acharya MM (2020) Mitigation of helium irradiation-induced brain injury by microglia depletion. J Neuroinflammation 17:159.

Andrásfalvy BK, Smith MA, Borchardt T, Sprengel R, Magee JC (2003) Impaired regulation of synaptic strength in hippocampal neurons from GluR1-deficient mice. J Physiol 552:35-45.

Andreas JJM, Kundapur V (2015) Hippocampus avoidance whole-brain radiation therapy: a practical intensity-modulated radiation therapy planning and delivery approach to RTOG 0933. J Med Imaging Radiat Sci 46:78-84.

Bartsch T, Wulff P (2015) The hippocampus in aging and disease: from plasticity to vulnerability. Neuroscience 309:1-16.

Bender ET (2012) Brain necrosis after fractionated radiation therapy: is the halftime for repair longer than we thought? Med Phys 39:7055-7061.

Blum S, Luchsinger JA, Manly JJ, Schupf N, Stern Y, Brown TR, DeCarli C, Small SA, Mayeux R, Brickman AM (2012) Memory after silent stroke: hippocampus and infarcts both matter. Neurology 78:38-46.

Boria AJ, Perez-Torres CJ (2019) Minimal difference between fractionated and single-fraction exposure in a murine model of radiation necrosis. Radiat Oncol 14:144.

Boria AJ, Perez-Torres CJ (2020) Impact of mouse strain and sex when modeling radiation necrosis. Radiat Oncol 15:141.

Brown PD, Gondi V, Pugh S, Tome WA, Wefel JS, Armstrong TS, Bovi JA, Robinson C, Konski A, Khuntia D, Grosshans D, Benzinger TLS, Bruner D, Gilbert MR, Roberge D, Kundapur V, Devisetty K, Shah S, Usuki K, Anderson BM, et al. (2020) Hippocampal avoidance during whole-brain radiotherapy plus memantine for patients with brain metastases: Phase III Trial NRG Oncology CC001. J Clin Oncol 38:1019-1029.

Cacao E, Cucinotta FA (2019) Meta-analysis of cognitive performance by novel object recognition after proton and heavy ion exposures. Radiat Res 192:463-472.

Caceres LG, Cid MP, Uran SL, Zorrilla Zubilete MA, Salvatierra NA, Guelman LR (2013) Pharmacological alterations that could underlie radiation-induced changes in associative memory and anxiety. Pharmacol Biochem Behav 111:37-43.

Chakraborti A, Allen A, Allen B, Rosi S, Fike JR (2012) Cranial irradiation alters dendritic spine density and morphology in the hippocampus. PLoS One 7:e40844.

Clarkson AN, Huang BS, Macisaac SE, Mody I, Carmichael ST (2010) Reducing excessive GABA-mediated tonic inhibition promotes functional recovery after stroke. Nature 468:305-309.

de Kruijff RM (2020) FLASH radiotherapy: ultra-high dose rates to spare healthy tissue. Int J Radiat Biol 96:419-423.

Duman JG, Dinh J, Zhou W, Cham H, Mavratsas VC, Paveškovic M, Mulherkar S, McGovern SL, Tolias KF, Grosshans DR (2018) Memantine prevents acute radiation-induced toxicities at hippocampal excitatory synapses. Neuro Oncol 20:655-665.

Fernandez F, Morishita W, Zuniga E, Nguyen J, Blank M, Malenka RC, Garner CC (2007) Pharmacotherapy for cognitive impairment in a mouse model of Down syndrome. Nat Neurosci 10:411-413.

Franco-Pérez J, Montes S, Sánchez-Hernández J, Ballesteros-Zebadúa P (2020) Whole-brain irradiation differentially modifies neurotransmitters levels and receptors in the hypothalamus and the prefrontal cortex. Radiat Oncol 15:269.

Galvin JE, Uryu K, Lee VM, Trojanowski JQ (1999) Axon pathology in Parkinson's disease and Lewy body dementia hippocampus contains alpha-, beta-, and gamma-synuclein. Proc Natl Acad Sci U S A 96:13450-13455.

Ge S, Pradhan DA, Ming GL, Song H (2007) GABA sets the tempo for activity-dependent adult neurogenesis. Trends Neurosci 30:1-8.

Gill KM, Lodge DJ, Cook JM, Aras S, Grace AA (2011) A novel α5GABA(A)R-positive allosteric modulator reverses hyperactivation of the dopamine system in the MAM model of schizophrenia. Neuropsychopharmacology 36:1903-1911.

Glasgow SD, Wong EW, Thompson-Steckel G, Marcal N, Séguéla P, Ruthazer ES, Kennedy TE (2020) Pre- and post-synaptic roles for DCC in memory consolidation in the adult mouse hippocampus. Mol Brain 13:56.

Gondi V, Tomé WA, Mehta MP (2010) Why avoid the hippocampus? A comprehensive review. Radiother Oncol 97:370-376.

Gong N, Li Y, Cai GQ, Niu RF, Fang Q, Wu K, Chen Z, Lin LN, Xu L, Fei J, Xu TL (2009) GABA transporter-1 activity modulates hippocampal theta oscillation and theta burst stimulation-induced long-term potentiation. J Neurosci 29:15836-15845.

Granger AJ, Shi Y, Lu W, Cerpas M, Nicoll RA (2013) LTP requires a reserve pool of glutamate receptors independent of subunit type. Nature 493:495-500.

Greene-Schloesser D, Moore E, Robbins ME (2013) Molecular pathways: radiation-induced cognitive impairment. Clin Cancer Res 19:2294-2300.
Han S, Tai C, Jones CJ, Scheuer T, Catterall WA (2014) Enhancement of inhibitory neurotransmission by GABAA receptors having α2,3-subunits ameliorates behavioral deficits in a mouse model of autism. Neuron 81:1282-1289.
Hinkle JJ, Olschowka JA, Love TM, Williams JP, O'Banion MK (2019) Cranial irradiation mediated spine loss is sex-specific and complement receptor-3 dependent in male mice. Sci Rep 9:18899.
Hodges H, Katzung N, Sowinski P, Hopewell JW, Wilkinson JH, Bywaters T, Rezvani M (1998) Late behavioural and neuropathological effects of local brain irradiation in the rat. Behav Brain Res 91:99-114.
Huang CS, Shi SH, Ule J, Ruggiu M, Barker LA, Darnell RB, Jan YN, Jan LY (2005) Common molecular pathways mediate long-term potentiation of synaptic excitation and slow synaptic inhibition. Cell 123:105-118.
Kopec CD, Real E, Kessels HW, Malinow R (2007) GluR1 links structural and functional plasticity at excitatory synapses. J Neurosci 27:13706-13718.
Krishnan B, Natarajan C, Bourne KZ, Alikhani L, Wang J, Sowa A, Groen K, Perry B, Dickstein DL, Baulch JE, Limoli CL, Britten RA (2021) Chronic low dose neutron exposure results in altered neurotransmission properties of the hippocampus-prefrontal cortex axis in both mice and rats. Int J Mol Sci 22:3668.
Lee SH, Lee KC, Choi J, Kim HY, Lee SH, Sung KH, Kim Y (2012) Clinical application of RapidArc volumetric modulated arc therapy as a component in whole brain radiation therapy for poor prognostic, four or more multiple brain metastases. Radiat Oncol J 30:53-61.
Leger M, Quiedeville A, Bouet V, Haelewyn B, Boulouard M, Schumann-Bard P, Freret T (2013) Object recognition test in mice. Nat Protoc 8:2531-2537.
Lissemore JI, Bhandari A, Mulsant BH, Lenze EJ, Reynolds CF, 3rd, Karp JF, Rajji TK, Noda Y, Zomorrodi R, Sibille E, Daskalakis ZJ, Blumberger DM (2018) Reduced GABAergic cortical inhibition in aging and depression. Neuropsychopharmacology 43:2277-2284.
Liu Y, Xiao S, Liu J, Zhou H, Liu Z, Xin Y, Suo WZ (2010) An experimental study of acute radiation-induced cognitive dysfunction in a young rat model. AJNR Am J Neuroradiol 31:383-387.
Makale MT, McDonald CR, Hattangadi-Gluth JA, Kesari S (2017) Mechanisms of radiotherapy-associated cognitive disability in patients with brain tumours. Nat Rev Neurol 13:52-64.
Malinow R, Malenka RC (2002) AMPA receptor trafficking and synaptic plasticity. Annu Rev Neurosci 25:103-126.
Manda K, Ueno M, Anzai K (2009) Cranial irradiation-induced inhibition of neurogenesis in hippocampal dentate gyrus of adult mice: attenuation by melatonin pretreatment. J Pineal Res 46:71-78.
Mann EO, Mody I (2010) Control of hippocampal gamma oscillation frequency by tonic inhibition and excitation of interneurons. Nat Neurosci 13:205-212.
McTyre E, Scott J, Chinnaiyan P (2013) Whole brain radiotherapy for brain metastasis. Surg Neurol Int 4:S236-244.
Milano MT, Grimm J, Niemierko A, Soltys SG, Moiseenko V, Redmond KJ, Yorke E, Sahgal A, Xue J, Mahadevan A, Muacevic A, Marks LB, Kleinberg LR (2021) Single- and multifraction stereotactic radiosurgery dose/volume tolerances of the brain. Int J Radiat Oncol Biol Phys 110:68-86.
Monje ML, Mizumatsu S, Fike JR, Palmer TD (2002) Irradiation induces neural precursor-cell dysfunction. Nat Med 8:955-962.
Montay-Gruel P, Acharya MM, Petersson K, Alikhani L, Yakkala C, Allen BD, Ollivier J, Petit B, Jorge PG, Syage AR, Nguyen TA, Baddour AAD, Lu C, Singh P, Moeckli R, Bochud F, Germond JF, Froidevaux P, Bailat C, Bourhis J, et al. (2019) Long-term neurocognitive benefits of FLASH radiotherapy driven by reduced reactive oxygen species. Proc Natl Acad Sci U S A 116:10943-10951.
Nicholson DA, Geinisman Y (2009) Axospinous synaptic subtype-specific differences in structure, size, ionotropic receptor expression, and connectivity in apical dendritic regions of rat hippocampal CA1 pyramidal neurons. J Comp Neurol 512:399-418.
Olpe HR, Steinmann MW, Ferrat T, Pozza MF, Greiner K, Brugger F, Froestl W, Mickel SJ, Bittiger H (1993) The actions of orally active GABAB receptor antagonists on GABAergic transmission in vivo and in vitro. Eur J Pharmacol 233:179-186.
Owonikoko TK, Arbiser J, Zelnak A, Shu HK, Shim H, Robin AM, Kalkanis SN, Whitsett TG, Salhia B, Tran NL, Ryken T, Moore MK, Egan KM, Olson JJ (2014) Current approaches to the treatment of metastatic brain tumours. Nat Rev Clin Oncol 11:203-222.
Parihar VK, Limoli CL (2013) Cranial irradiation compromises neuronal architecture in the hippocampus. Proc Natl Acad Sci U S A 110:12822-12827.
Patterson MA, Szatmari EM, Yasuda R (2010) AMPA receptors are exocytosed in stimulated spines and adjacent dendrites in a Ras-ERK-dependent manner during long-term potentiation. Proc Natl Acad Sci U S A 107:15951-15956.
Pellmar TC, Schauer DA, Zeman GH (1990) Time- and dose-dependent changes in neuronal activity produced by X radiation in brain slices. Radiat Res 122:209-214.
Peng Y, Lu K, Li Z, Zhao Y, Wang Y, Hu B, Xu P, Shi X, Zhou B, Pennington M, Chandy KG, Tang Y (2014) Blockade of Kv1.3 channels ameliorates radiation-induced brain injury. Neuro Oncol 16:528-539.
Pontes A, Zhang Y, Hu W (2013) Novel functions of GABA signaling in adult neurogenesis. Front Biol (Beijing) 8:10.
Rao AA, Ye H, Decker PA, Howe CL, Wetmore C (2011) Therapeutic doses of cranial irradiation induce hippocampus-dependent cognitive deficits in young mice. J Neurooncol 105:191-198.
Rivera PD, Shih HY, Leblanc JA, Cole MG, Amaral WZ, Mukherjee S, Zhang S, Lucero MJ, Decarolis NA, Chen BP, Eisch AJ (2013) Acute and fractionated exposure to high-LET (56)Fe HZE-particle radiation both result in similar long-term deficits in adult hippocampal neurogenesis. Radiat Res 180:658-667.
Roobol SJ, van den Bent I, van Cappellen WA, Abraham TE, Paul MW, Kanaar R, Houtsmuller AB, van Gent DC, Essers J (2020) Comparison of high- and low-LET radiation-induced DNA double-strand break processing in living cells. Int J Mol Sci 21:6602.
Sando R, Bushong E, Zhu Y, Huang M, Considine C, Phan S, Ju S, Uytiepo M, Ellisman M, Maximov A (2017) Assembly of Excitatory Synapses in the Absence of Glutamatergic Neurotransmission. Neuron 94:312-321.e3.
Schulz JM, Knoflach F, Hernandez MC, Bischofberger J (2019) Enhanced dendritic inhibition and impaired NMDAR activation in a mouse model of Down syndrome. J Neurosci 39:5210-5221.
Semmler A, Garbe S, Moskau S, Frisch C, Eter N, Schlegel U, Linnebank M (2013) An efficient method for fractionated whole rodent brain radiation. Neurol Res 35:355-359.
Shepherd JD, Huganir RL (2007) The cell biology of synaptic plasticity: AMPA receptor trafficking. Annu Rev Cell Dev Biol 23:613-643.
Shi L, Adams MM, Long A, Carter CC, Bennett C, Sonntag WE, Nicolle MM, Robbins M, D'Agostino R, Brunso-Bechtold JK (2006) Spatial learning and memory deficits after whole-brain irradiation are associated with changes in NMDA receptor subunits in the hippocampus. Radiat Res 166:892-899.
Sokolova IV, Schneider CJ, Bezaire M, Soltesz I, Vlkolinsky R, Nelson GA (2015) Proton radiation alters intrinsic and synaptic properties of CA1 pyramidal neurons of the mouse hippocampus. Radiat Res 183:208-218.
Son Y, Yang M, Wang H, Moon C (2015) Hippocampal dysfunctions caused by cranial irradiation: a review of the experimental evidence. Brain Behav Immun 45:287-296.
Titley HK, Brunel N, Hansel C (2021) Toward a Neurocentric View of Learning. Neuron 95:19-32.
Tolliver JM, Pellmar TC (1987) Ionizing radiation alters neuronal excitability in hippocampal slices of the guinea pig. Radiat Res 112:555-563.
von Oertzen J, Urbach H, Blümcke I, Reuber M, Träber F, Peveling T, Menzel C, Elger CE (2002) Time-efficient T2 relaxometry of the entire hippocampus is feasible in temporal lobe epilepsy. Neurology 58:257-264.
Vorhees CV, Williams MT (2006) Morris water maze: procedures for assessing spatial and related forms of learning and memory. Nat Protoc 1:848-858.
Wang TM, Shen GP, Chen MY, Zhang JB, Sun Y, He J, Xue WQ, Li XZ, Huang SY, Zheng XH, Zhang SD, Hu YZ, Qin HD, Bei JX, Ma J, Mu J, Yao Shugart Y, Jia WH (2019) Genome-wide association study of susceptibility loci for radiation-induced brain injury. J Natl Cancer Inst 111:620-628.
Wang P, Sui HJ, Li XJ, Bai LN, Bi J, Lai H (2021) Melatonin ameliorates microvessel abnormalities in the cerebral cortex and hippocampus in a rat model of Alzheimer's disease. Neural Regen Res 16:757-764.
Wang X, Meng ZX, Chen YZ, Li YP, Zhou HY, Yang M, Zhao TT, Gong YL, Wu Y, Liu T (2020) Enriched environment enhances histone acetylation of NMDA receptor in the hippocampus and improves cognitive dysfunction in aged mice. Neural Regen Res 15:2327-2334.
Wu PH, Coultrap S, Pinnix C, Davies KD, Tailor R, Ang KK, Browning MD, Grosshans DR (2012) Radiation induces acute alterations in neuronal function. PLoS One 7:e37677.
Xu P, Xu Y, Hu B, Wang J, Pan R, Murugan M, Wu LJ, Tang Y (2015) Extracellular ATP enhances radiation-induced brain injury through microglial activation and paracrine signaling via P2X7 receptor. Brain Behav Immun 50:87-100.
Xue NY, Ge DY, Dong RJ, Kim HH, Ren XJ, Tu Y (2021) Effect of electroacupuncture on glial fibrillary acidic protein and nerve growth factor in the hippocampus of rats with hyperlipidemia and middle cerebral artery thrombus. Neural Regen Res 16:137-142.
Yang L, Yang J, Li G, Li Y, Wu R, Cheng J, Tang Y (2017) Pathophysiological responses in rat and mouse models of radiation-induced brain injury. Mol Neurobiol 54:1022-1032.
Zamanillo D, Sprengel R, Hvalby O, Jensen V, Burnashev N, Rozov A, Kaiser KM, Köster HJ, Borchardt T, Worley P, Lübke J, Frotscher M, Kelly PH, Sommer B, Andersen P, Seeburg PH, Sakmann B (1999) Importance of AMPA receptors for hippocampal synaptic plasticity but not for spatial learning. Science 284:1805-1811.
Zanni G, Deutsch HM, Rivera PD, Shih HY, LeBlanc JA, Amaral WZ, Lucero MJ, Redfield RL, DeSalle MJ, Chen BPC, Whoolery CW, Reynolds RP, Yun S, Eisch AJ (2018) Whole-Body (12)C Irradiation transiently decreases mouse hippocampal dentate gyrus proliferation and immature neuron number, but does not change new neuron survival rate. Int J Mol Sci 19:3078.
Zhang D, Zhou W, Lam TT, Weng C, Bronk L, Ma D, Wang Q, Duman JG, Dougherty PM, Grosshans DR (2018) Radiation induces age-dependent deficits in cortical synaptic plasticity. Neuro Oncol 20:1207-1214.
Zou WJ, Song YL, Wu MY, Chen XT, You QL, Yang Q, Luo ZY, Huang L, Kong Y, Feng J, Fang DX, Li XW, Yang JM, Mei L, Gao TM (2020) A discrete serotonergic circuit regulates vulnerability to social stress. Nat Commun 11:4218.
Zou Y, Corniola R, Leu D, Khan A, Sahbaie P, Chakraborti A, Clark DJ, Fike JR, Huang TT (2012) Extracellular superoxide dismutase is important for hippocampal neurogenesis and preservation of cognitive functions after irradiation. Proc Natl Acad Sci U S A 109:21522-21527.
Zurek AA, Yu J, Wang DS, Haffey SC, Bridgwater EM, Penna A, Lecker I, Lei G, Chang T, Salter EW, Orser BA (2014) Sustained increase in α5GABAA receptor function impairs memory after anesthesia. J Clin Invest 124:5437-5441.

C-Editor: Zhao M; S-Editors: Yu J, Li CH; L-Editors: Yu J, Song LP; T-Editor: Jia Y